

MATHEMATICAL MODELLING OF FROST LAYER GROWTH
IN A FIN-AND-TUBE HEAT EXCHANGER

Kristian Lenic, Anica Trp, Bernard Frankovic

Faculty of Engineering University of Rijeka,
Rijeka, Vukovarska 58, Croatia
kristian.lenic@riteh.hr, anica.trp@riteh.hr, bernard.frankovic@riteh.hr

In the paper a numerical analysis of heat and mass transfer during frost formation on a fin-and-tube heat exchanger has been performed. Frost layer formation significantly influences the heat transfer on heat exchanger fins. The numerical analysis of the frost growth enables predictions of the heat transfer resistance and the decrease of exchanged heat flux. A transient two-dimensional mathematical model of frost formation has been developed. The applied mathematical model has been defined using governing equations for the boundary layer that include air and frost sub-domains as well as a boundary condition on the air-frost interface. The mathematical model with initial and boundary conditions has been discretised according to the finite volume method and solved numerically using SIMPLER algorithm for the velocity-pressure coupling. As result of numerical calculations, time-wise frost thickness variations for different air humidities have been presented.

INTRODUCTION

Frost layer formation is an important consideration in the field of refrigeration and air-conditioning. This paper deals with the frost formation on finned surfaces of fin-and tube heat exchanger when fin surface temperature falls below the temperature of water freezing.

Frost formation on heat exchanger surfaces extremely influences the heat transfer since the porous structure of frost layers acts as an thermal insulator. Moreover, accumulations of the frost layer often become thick enough to restrict air flow. The thermal resistance of frost layer and reduction of air flow due to augmented pressure drop causes significant decreasing of heat exchanger efficiency. This has an effect on space cooling quality and working behaviour of whole device. The principal aim of frost formation analysis is estimation of exchanged heat flux under transient conditions of augmented thermal resistance.

The thermal conductivity of the frost layer depends on several parameters such us the temperature at which frost layer forms, density of frost layer, etc. The porous structure of frost layer consists of ice crystals and air gaps. Whereas frost layer contains air pores with low thermal conductivity the whole frost layer represents significant thermal resistance.

The majority of models developed so far can be classified into several groups. One is the group of models which predict the variations of frost properties from the diffusion equation

applied to the frost layer and then calculate the amount of heat and mass transfer in the frost layer by using the correlations on the air-side. This approach is used by Lee et al.(1997), Jones et al. (1975), Sahin (1995) and Cheng (2001). The second group of modelling methods gives some improvements and analyzes the air flow with boundary layer equations and predicts the frost properties by using the correlations. Lee et al.(2003) developed a mathematical model without using the correlations for air boundary layer zone and frost layer zone. Le Gall et al. (1997) developed a transient one-dimensional model for frost growth and frost density changes formed on cooled surface in the humid air stream. Lürer and Beer (2000) theoretically and experimentally investigated the frost formation process on parallel plates in humid air stream in laminar flow. Na and Weeb (2004) investigated basic phenomena related with frost layer formation and growth. They experimentally measured water vapour mass flux from air stream to frost layer. By analysis of measured data they stated that the partial pressure of water vapour on frost layer surface is greater than partial pressure of water vapour for the temperature of frost layer surface, i.e. that air near the surface of frost layer is supersaturated.

In this paper a calculation of air velocity, temperature and humidity fields have been performed allowing more exact description of heat and mass transfer. Furthermore, the problem has been solved as a transient and two-dimensional. In the presented mathematical model some latest acquisitions from previous models have been introduced. Detailed approach could be found in Lenic (2006).

MATHEMATICAL MODEL

Domain of calculation includes one half of space between fins, as presented on Fig. 1. Domain consists of two subdomains: subdomain of humid air and subdomain of frost layer which are delimited by air-frost interface.

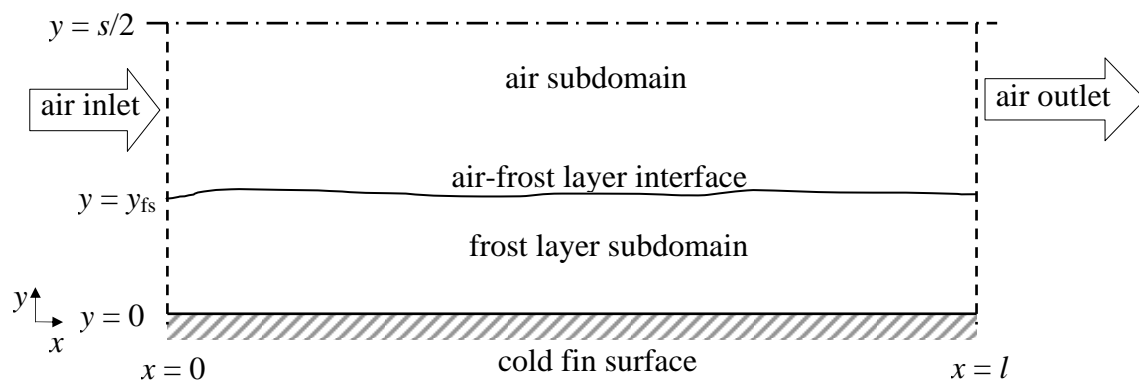


Fig. 1. Domain of numerical calculation

Governing equations, initial and boundary conditions

For the air subdomain heat and mass flow have been described using continuity, momentum and energy equations as well as water vapour transport equation. For the frost layer subdomain energy equation and modified diffusion equation have been used. Initial and boundary conditions have been given in Table 1. and Table 2.

Air subdomain

$$\frac{\partial}{\partial x}(\rho_a u_x) + \frac{\partial}{\partial y}(\rho_a u_y) = 0 \quad (1)$$

$$\rho_a \frac{\partial u_x}{\partial t} + \rho_a \left(u_x \frac{\partial u_x}{\partial x} + u_y \frac{\partial u_x}{\partial y} \right) = -\frac{\partial p}{\partial x} + \eta \left(\frac{\partial^2 u_x}{\partial x^2} + \frac{\partial^2 u_x}{\partial y^2} \right) \quad (2)$$

$$\rho_a \frac{\partial u_y}{\partial t} + \rho_a \left(u_x \frac{\partial u_y}{\partial x} + u_y \frac{\partial u_y}{\partial y} \right) = -\frac{\partial p}{\partial y} + \eta \left(\frac{\partial^2 u_y}{\partial x^2} + \frac{\partial^2 u_y}{\partial y^2} \right) \quad (3)$$

$$\rho_a \frac{\partial \mathcal{G}_a}{\partial t} + \rho_a \cdot \left(u_x \frac{\partial \mathcal{G}_a}{\partial x} + u_y \frac{\partial \mathcal{G}_a}{\partial y} \right) = \frac{\lambda_a}{c_{p,a}} \left(\frac{\partial^2 \mathcal{G}_a}{\partial x^2} + \frac{\partial^2 \mathcal{G}_a}{\partial y^2} \right) \quad (4)$$

$$\rho_a \frac{\partial w}{\partial t} + \rho_a \cdot \left(u_x \frac{\partial w}{\partial x} + u_y \frac{\partial w}{\partial y} \right) = \rho_a \cdot D \cdot \left(\frac{\partial^2 w}{\partial x^2} + \frac{\partial^2 w}{\partial y^2} \right) \quad (5)$$

Frost layer subdomain

$$\rho_{fl} \frac{\partial \mathcal{G}_{fl}}{\partial t} = \frac{\partial}{\partial x} \left(\frac{\lambda_{fl}}{c_{p,fl}} \frac{\partial \mathcal{G}_{fl}}{\partial x} \right) + \frac{\partial}{\partial y} \left(\frac{\lambda_{fl}}{c_{p,fl}} \frac{\partial \mathcal{G}_{fl}}{\partial y} \right) + q_{sub} \frac{\partial \rho_{ls}}{\partial t} \quad (6)$$

$$\frac{\partial \rho_{fl}}{\partial t} = \frac{\partial}{\partial x} \left(D_{eff} \rho_a \frac{\partial (\rho_v / \rho_a)}{\partial x} \right) + \frac{\partial}{\partial y} \left(D_{eff} \rho_a \frac{\partial (\rho_v / \rho_a)}{\partial y} \right) \quad (7)$$

Table 1. Initial and boundary conditions

Initial condition $t = 0$	$0 < y < y_{fs}$	$\mathcal{G}_{fl0} = \mathcal{G}_s, \rho_{fl0} = 30 \text{ kg/m}^3$
	$y_{fs} < y < s/2$	$u_{x0} = 0, u_{y0} = 0, \mathcal{G}_{z0} = \mathcal{G}_{in}, w_0 = w_{in}$
Boundary conditions $t > 0$		
left (inlet) boundary $x = 0, 0 < y < s/2$	$0 < y < y_{fs}$	$\frac{\partial \mathcal{G}_{fl}}{\partial x} = 0, \frac{\partial (\rho_v / \rho_a)}{\partial x} = 0$
	$y_{fs} < y < s/2$	$u_x = u_{in}, u_y = 0, \mathcal{G}_z = \mathcal{G}_{in}, w = w_{in}$
top boundary $0 < x < l, y = s/2$		$u_y = 0, \frac{\partial u_x}{\partial y} = 0, \frac{\partial \mathcal{G}_a}{\partial y} = 0, \frac{\partial w}{\partial y} = 0$
right (outlet) boundary $x = l, 0 < y < s/2$	$0 < y < y_{fs}$	$\frac{\partial \mathcal{G}_{fl}}{\partial x} = 0, \frac{\partial (\rho_v / \rho_a)}{\partial x} = 0$
	$y_{fs} < y < s/2$	$\frac{\partial u_x}{\partial x} = 0, \frac{\partial u_y}{\partial x} = 0, \frac{\partial \mathcal{G}_z}{\partial x} = 0, \frac{\partial w}{\partial x} = 0$
bottom boundary $0 < x < l, y = 0$		$\mathcal{G}_{fl} = \mathcal{G}_s, \frac{\rho_v}{\rho_a} = \frac{\rho_v(\mathcal{G}_s)}{\rho_a(\mathcal{G}_s)}$

Table 2. Boundary conditions at the air-frost interface

Air-frost layer interface $0 < x < l, y = y_{fs}$	$u_x = 0, u_y = 0,$ $w_{fs} = 0.622 \cdot \frac{(1+S)p_{v,sat}}{p - (1+S_v)p_{v,sat}}, S = 0.808 \left(\frac{p_{v,\infty}}{p_{v,sat,\infty}} \right) \left(\frac{p_{v,sat,fs}}{p_{v,sat,\infty}} \right)^{-0.657} - 1$ $\lambda_a \frac{\partial g_a}{\partial y} = \lambda_{fl} \frac{\partial g_{fl}}{\partial y} + q_{sub} \rho_{fl} \frac{dy_{fl}}{dt}, \frac{\partial \rho_{fl}}{\partial y} = 0$
---	--

Velocity of frost surface moving

Frost formation process depends on water vapour transfer from air stream into frost layer, diffusion rate of water vapour into the frost layer and thermal conduction inside the layer. One part of water vapour flux which transfers from the air stream have been deposited on frost surface and increases the frost thickness. The other part of water vapour flux enters inside the frost layer and thus increases its density. Accuracy of determination of water mass flux which enters inside the frost layer has crucial influence on accuracy of determination of frost layer growth rate. The total mass flux of water vapour transferring from air to frost layer surface and mass flux which increases the frost layer density absorbed into frost layer are defined respectively as follows:

$$\dot{m}_a = \rho_a \cdot D \cdot \frac{dw}{dy}, \dot{m}_{diff} = -\rho_a \cdot D_{eff} \cdot \frac{d(\rho_v/\rho_a)}{dy} \quad (8)$$

The difference of these mass fluxes equals the quantity of water (ice) which has been deposited on layer surface. Consequently the mass flux responsible for layer thickness growth is

$$\dot{m}_{\Delta y} = \rho_{fl} \frac{dy_{fl}}{dt} = \dot{m}_a - \dot{m}_{diff} \quad (9)$$

Follows the frost layer growth rate:

$$\frac{dy_{ls}}{dt} = \frac{1}{\rho_{ls}} \dot{m}_{\Delta y} = \frac{1}{\rho_{ls}} (\dot{m}_a - \dot{m}_{diff}) \quad (10)$$

Physical properties of frost layer

The effective thermal conductivity, the specific heat and effective diffusion coefficient of the frost layer have been calculate using following equations:

$$\lambda_{fl} = 0,132 + 3,13 \cdot 10^{-4} \rho_{fl} + 1,6 \cdot 10^{-7} \rho_{fl}^2 \quad (11)$$

$$c_{p,fl} = \frac{1}{\rho_{fl}} [\rho_i (1 - \varepsilon) c_{p,i} + \rho_a \varepsilon c_{p,a}] \quad (12)$$

$$D_{eff} = D \cdot \varepsilon \cdot \tau = D \cdot \varepsilon \cdot \frac{1 + \varepsilon}{2}, \tau = \frac{1 + \varepsilon}{2} \quad (13)$$

NUMERICAL SOLVING

The governing equations are discretised according finite volume method. The convection-diffusion terms have been discretised using power-law scheme and the resulting set of linearised discretisation equations have been solved using an iterative procedure. A fully implicit method has been used for time-stepping treatment. For the velocity-pressure coupling the SIMPLER algorithm has been applied (Patankar, 1980). Algorithm has been implemented in a self-written FORTRAN code and solved on a personal computer (2,6 GHz). Detailed description of numerical approach have been given in Lenic (2006).

EXPERIMENTAL VALIDATION

The experimental validation of the numerical model and developed computer code have been performed. Inlet conditions during the experimental investigation have been used as input data in numerical simulations.

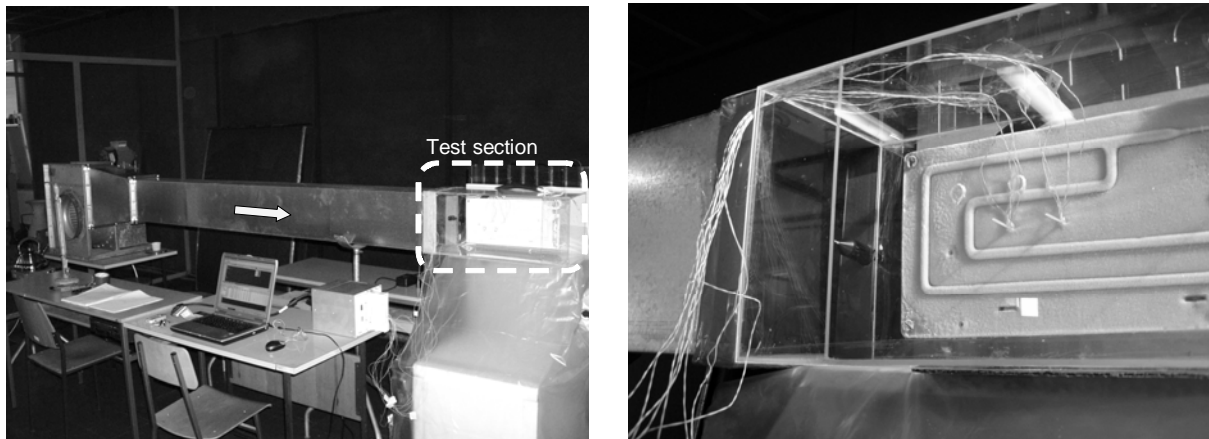


Fig. 2. Experimental unit and test section

An experimental test section consisted of an aluminium cooled plate placed in a humid air stream with controlled inlet conditions, Fig. 2. Time-wise frost layer thickness variations with comparison of numerical and experimental data are shown in Fig. 3.

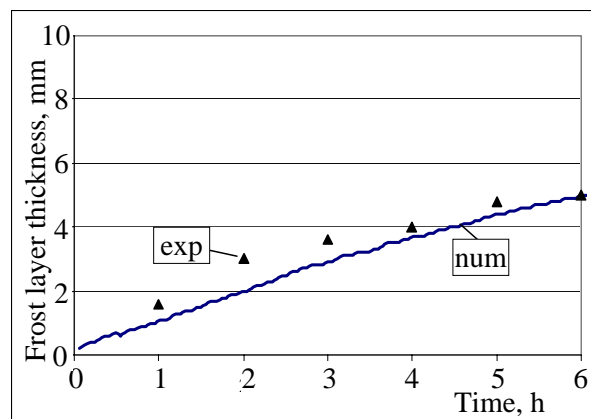


Fig. 3. Time-wise frost layer thickness variations – comparison of experimental and numerical values ($\vartheta_{a,in} = 21.4 \text{ }^\circ\text{C}$, $w_{in} = 0.0062 \text{ kg/kg}$, $u_{x,in} = 0.6 \text{ m/s}$, $\vartheta_{fs} = -19.5 \text{ }^\circ\text{C}$)

RESULTS

Frost growth rate

After the validation of mathematical model and computer code, the numerical analysis have been performed for fin-and-tube heat exchanger with following geometrical characteristics: fin thickness 0.001 m, space between fins 0.006 m, fins width 0.048 m, total number of pipes 189, total number of fins 210, heat exchanger surface 18 m², longitudinal pipe distance 0.016 m, transversal pipe distance 0.014 m, outer pipe diameter 0.01 m and inside pipe diameter 0.008 m. A set of numerical calculation has been performed in order to evaluate the influence of inlet air velocity, temperature and humidity on the frost growth rate. Numerical analysis has been carried out for different inlet air velocities, temperatures and humidity. Time-wise frost layer thickness variation for different air humidity and different air temperatures have been shown on Fig. 4 and 5.

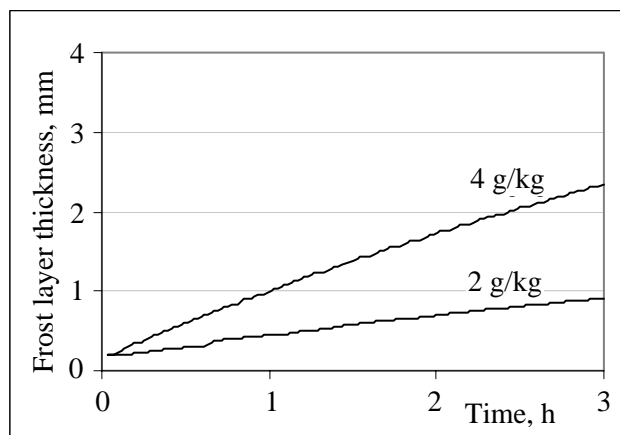


Fig. 4. Time-wise frost layer thickness variation for different air humidity and inlet air temperature of 5 °C ($u_{x,in} = 1$ m/s, $\vartheta_{fs} = -12$ °C)

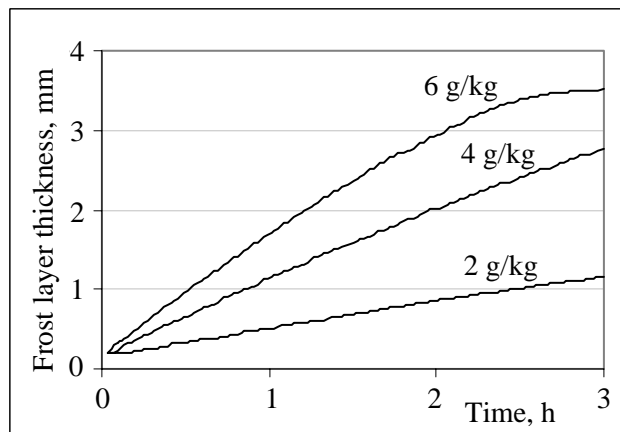


Fig. 5. Time-wise frost layer thickness variation for different air humidity and inlet air temperature of 12 °C ($u_{x,in} = 1$ m/s, $\vartheta_{fs} = -12$ °C)

Frost layer growth is more intensive under the higher air humidity because of higher gradient of air humidity near the frost surface in the boundary layer. This influence of air humidity on frost layer growth rate is substantial.

CONCLUSIONS

Investigations described in this paper have included numerical and experimental analyses of heat and mass transfer during frost formation on a fin-and-tube heat exchanger. Results have shown that phenomena of frost formation on a cold surface placed in a humid air stream requires a complex mathematical approach. The numerical analysis should take into account the porous nature of the frost layer and appropriate physical properties have to be calculated.

It can be concluded that the frost layer growth is faster when the inlet air humidity and inlet air temperature are higher. Frost layer formation significantly influences the heat transfer from air to refrigerant which evaporates inside the heat exchanger pipes. Using a developed mathematical model, algorithm and computer code, which have been experimentally validated, it is possible to predict a decrease of exchanged heat flux in heat exchanger under the frost growth conditions.

Investigations have been performed as a part of the scientific project *Research and development of renewable energy components and systems* financed by Ministry of Science, Education and Sports of the Republic of Croatia.

LIST OF SYMBOLS

c_p	specific heat under constant pressure ($\text{J kg}^{-1} \text{K}^{-1}$)
D	diffusivity ($\text{m}^2 \text{s}^{-1}$)
l	domain length (m)
\dot{m}	water vapour mass flux ($\text{kg m}^{-2} \text{s}^{-1}$),
p	pressure (Pa)
q	specific heat of sublimation (J kg^{-1})
S	supersaturation degree
s	distance between fins (m)
t	time (s)
u_x	x-velocity component (m s^{-1})
u_y	y-velocity component (m s^{-1})
w	mass fraction of water vapour in air (kg kg^{-1})
x	coordinate (m)
y	coordinate (m)

Greek symbols

ε	porosity
η	dynamic viscosity ($\text{kg s}^{-1} \text{m}^{-1}$)
ϑ	temperature ($^{\circ}\text{C}$)
λ	thermal conductivity, ($\text{W m}^{-1} \text{K}^{-1}$)
ρ	density (kg m^{-3})
τ	tortuosity factor

Subscripts

a	air
diff	related to diffusion into frost layer
eff	effective
fl	frost layer
fs	frost surface

i	ice
in	inlet
s	fin surface
sat	saturated
v	water vapour
Δy	related to layer thickness increasing
0	initial value

LITERATURE

Cheng, C.H. and Cheng Y.C., 2001, Predictions of frost growth on a cold plate in atmospheric air, *International Comm. Heat and Mass Transfer*, Vol. 28, pp. 963-962.

Jones, B. W. and Parker, J. D., 1975, Frost formation with varying environmental parameters, *Journal of Heat Transfer*, Vol. 97, pp. 255-259.

Le Gall, R., Grillot, J. M. and Jallut, C., 1997, Modelling of frost growth and densification, *International Journal of Heat and Mass Transfer*, Vol. 40, pp. 3177-3187.

Lee, K. S., Kim, W. S. and Lee, T. H., 1997, A one-dimensional model for frost formation on a cold surface, *International Journal of Heat and Mass Transfer*, Vol. 40, pp. 4359-4365.

Lee, K., Jhee, S. and Yang, D., 2003, Prediction of the frost formation on a cold flat surface, *International Journal of Heat and Mass Transfer*, Vol. 46, pp. 3789-3796.

Lenic, K., 2006, Analysis of heat and mass transfer during frost formation on fin-and-tube heat exchangers, Ph.D. Dissertation, Faculty of Engineering, University of Rijeka, Rijeka, Croatia, (in Croatian).

Lüer, A., Beer, H., 2000, Frost deposition in a parallel plate channel under laminar flow conditions, *International Journal of Thermal Science*, Vol. 39, pp. 85-95,

Na, B. and Weeb, R. L., 2004, New model for frost growth rate, *International Journal of Heat and Mass Transfer*, Vol. 47, pp. 925-936.

Na, B., and Weeb, R. L., 2004, Mass transfer on and within a frost layer, *International Journal of Heat and Mass Transfer*, Vol. 47, pp. 899-911.

Patankar, S. V., 1980, *Numerical Heat Transfer and Fluid Flow*, Hemisphere Publishing Corporation, Taylor & Francis Group, New, York.

Sahin, A. Z., 1995, An analytical study of frost nucleation and growth during the crystal growth period, *International Journal of Heat and Mass Transfer*, Vol. 30, pp. 321-330.